Synthesis of Volcanic Ash-based Geopolymer Mortar Designed by the Taguchi Method

Rahmi Karolina [1*], Johannes Tarigan [1], M. A. Megat Johari [2], M. J. A. Mijarsh [3], Harianto Hardjasaputra [4]

[1] Civil Engineering Department, Faculty of Engineering, Universitas Sumatera Utara, Indonesia.

[2] School of Civil Engineering, Universiti Sains Malaysia, Malaysia.

[3] Civil Engineering Department, Faculty of Engineering, Al-Merghab University, Al-Khums, Libya.

[4] Civil Engineering Department, Faculty of Engineering, Universitas Pembangunan Jaya, Banten, Indonesia.

Abstract

This study focuses on the geopolymer synthesized from Mount Sinabung's volcanic ash. The compressive strength of the geopolymer was determined by optimizing five factors using the Taguchi method's L16 array. The five factors included: volcanic ash wt.%, Sodium silicate (Na_2SiO_3) wt.%, Sodium hydroxide (NaOH) concentration (mole), Na2SiO3/NaOH wt.% and water/binder (w/b) wt.%. A total of 16 mixtures were prepared per the L16 array and evaluated on five levels to obtain the optimum mixture. The main findings of this study revealed that A2B1C2D3E4 produced the highest compressive strength of 79.625 MPa after three days of curing time, while A4B2C3D1E4 produced the lowest compressive strength of 41.93 MPa. The signal-to-noise (S/N) ratio analysis from the Taguchi method shows that the factor of Na2SiO3 has a greater impact on compressive strength. The X-ray diffraction (XRD) result for the geopolymer mortar revealed the formation of aluminosilicate type (N-A-S-H) and calcium silicate (C-S-H) gels, whereas the Scanning Electron Microscopy (SEM) result exhibited numerous pores and a denser structure. These characterization results demonstrated that the polymerization of volcanic ash mortar from Sinabung successfully conserves natural resources.

Keywords: Compressive Strength; Geopolymer; Taguchi Method; Volcanic Ash.

1. Introduction

The main material in the construction industry is Portland cement, which emits 5-8% CO_2 during production and 70% during concrete manufacturing [1–3]. This material is regarded as a significant source of carbon emissions, prompting researchers to advocate for the elimination of Portland cement to combat global warming [4–6]. An innovative geopolymer technology created by Gilikhovsky and subsequently developed by Davidovits has piqued the interest of researchers worldwide as a potential alternative cement binder [7, 8]. Geopolymers, an inorganic polymer, have recently been identified as a next-generation building material because their production reduces CO_2 emissions significantly compared to Portland cement [9, 10]. Geopolymer is produced by polymer interaction between alkaline solutions based on sodium silicate (Na_2SiO_3) wt.% or sodium hydroxide (NaOH) and metallic ions obtained from active fillers, primarily Al^{3+} and Si^{4+} [11, 12]. Consequently, the increased amount of aluminosilicate minerals is an important aspect of the geopolymer manufacturing process.

The presence of abundant elements such as Si and Al satisfies the requirements for a cement replacement. Due to the abundance of aluminosilicate minerals, the use of fly ash, metakaolin (MK), calcined kaolin, and ground granulated blast furnace slag (GGBFS) as active fillers has become increasingly common [13,14]. However, these essential minerals are obtained through the recycling process and the disposal of industrial and construction waste, which limits the availability of these resources [15]. Due to the sustainability and availability of natural resources, volcanic ash is regarded as a potential resource for overcoming the limitations of industrial waste material. Mount Sinabung is one of Indonesia's active volcanoes, spewing up black and thick smoke followed by sand and a deluge of volcanic ash since November 2013. Several references, however, confirmed that volcanic ash had similar differences between SiO_2 and Al_2O_3 concentrations to GGBFS, MK, and class F and C fly ash, making it a suitable choice [16–18]. The total aluminosilicate concentration of the raw materials correlates directly with geopolymerization outcomes. It may be described that silica improved the geopolymer's strength, thereby increasing the bonding density of Si-O-Si [19–21]. Consequently, the high concentration of aluminosilicate minerals and the abundance of volcanic ash in Sinabung reveal a crucial raw material for synthesizing geopolymers.

In this study, the type of alkaline activator was determined as a critical parameter affecting the geopolymerization of Sinabung volcanic ash. The most common types include NaOH, Na_2SiO_3, and a mixture of the two chemicals ($NaOH/Na_2SiO_3$), which are considered based on previous research [22, 23]. However, researchers are yet to offer a conclusive explanation of the impacts of alkaline activators, such as how strength increases with a higher concentration of Na_2SiO_3, NaOH, or a higher concentration of the $Na_2SiO_3/NaOH$ ratio and vice versa [24, 25]. To that end, adding an alkaline activator to the geopolymerization of Sinabung volcanic ash was investigated in this study using the Taguchi method to determine each type of alkaline contribution to the compressive strength result.

The purpose of the alkaline activator's contribution to compressive strength was determined using the Taguchi method. This method is a viable design method for evaluating five factors in a single work, namely, the volcanic ash weight percentage, the Na_2SiO_3 weight percentage, the NaOH concentration (mole), the $Na_2SiO_3/NaOH$ weight percentage, and the water/binder (w/b) weight percentage [4, 26]. The optimal combination was examined utilizing the Taguchi method's L16 array, whereby the five parameters were experimented with on four levels, resulting in 13 trials. The factors above were examined based on compressive strengths for various Sinabung volcanic ash mortars. In addition, signal-to-noise (SN) ratio analyses were used to determine the factors with the greatest and least impact on compressive strength. The highest compressive strength mortar was subsequently characterized using X-ray Diffraction and Scanning Electron Microscopy instruments to investigate the correlation between compressive strength and geopolymerization of volcanic ash.

2. Materials and Methods

Figure 1 depicts a flowchart summarizing the entire collection of experimental research conducted in this study. This design guided the synthesis of a suitable geopolymer mortar with adequate strength and performance.
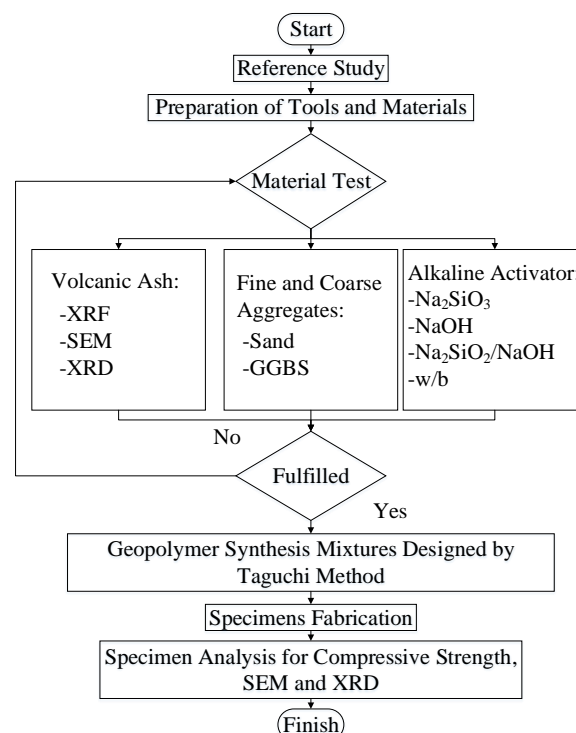

Figure 1. The flowchart of experimental research

2.1. Materials

In this investigation, volcanic ash from Indonesia's Sinabung Mountain served as the primary component of the concrete manufacturing process. Table 1 summarizes the XRF-determined chemical composition of volcanic ash. Among dominant chemical compounds, the highest amount of 38.8% was produced from SiO_2, while Al_2O_3 and Fe_2O_3 exhibited 13.1% and 6.8%, respectively. In addition, particle size distributions were measured with the Particle Size Analyzer (PSA) – Fritsch Analysette 22, for which Figure 2 displays a grading curve. Meanwhile, sand in the form of fine aggregate was utilized with apparent specific gravity values of 2.59 and a fineness modulus of 2.54. Analytical grade sodium hydroxide (NaOH), sodium silicate (Na_2SiO_3) with a 40% concentration in liquid form, and a mixture of the two chemicals Na_2SiO^3/NaOH were employed as alkaline activators.

Table 1. Chemical composition using XRF technique from Sinabung volcanic ash

Component	Result	Unit
SiO_2	38.8137	mass%
Al_2O_3	12.0467	mass%
Fe_2O_3	6.8549	mass%
CaO	4.4284	mass%
K_2O	2.1075	mass%
SO_3	2.0114	mass%
TiO_2	0.6152	mass%
MgO	0.2678	mass%
P_2O_5	0.2124	mass%
MnO	0.1365	mass%
SrO	0.0407	mass%
Cl	0.033	mass%
ReO_2	0.0294	mass%
ZrO_2	0.0219	mass%
As_2O_3	0.0202	mass%
Rb_2O	0.0076	mass%
Balance	32.3527	mass%
Total	100	mass%
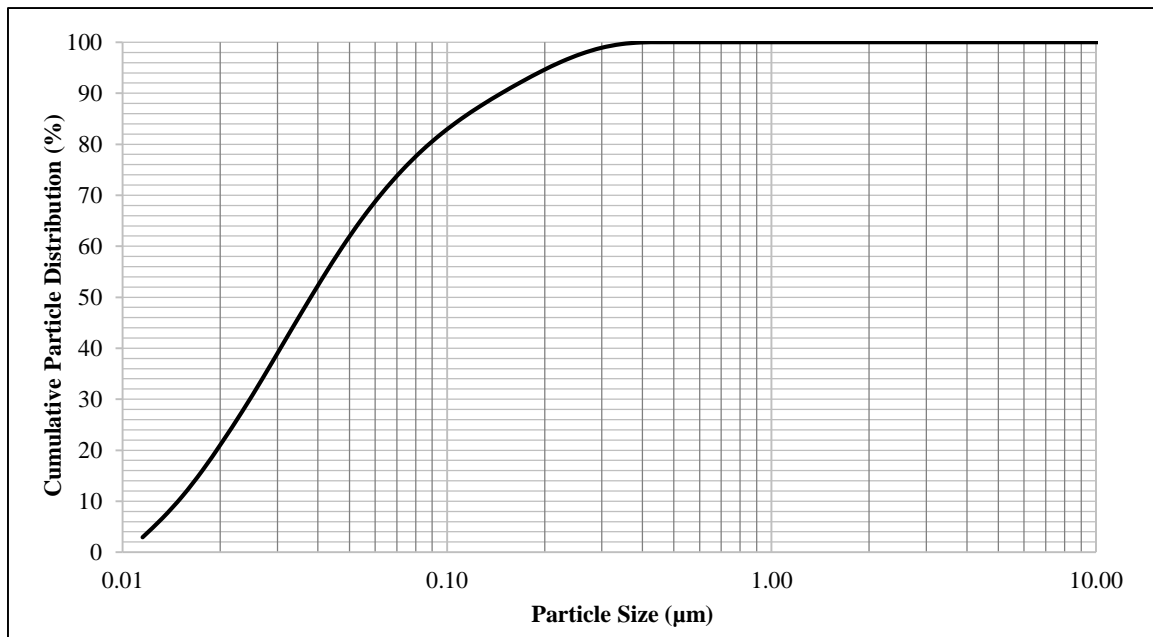
Figure 2. Grading curves for Sinabung volcanic ash

2.2. Determination of Optimal Mixtures

The Taguchi method was employed to identify the best mixtures based on the impact of critical factors on mechanical characteristics. Five major factors were studied, including a statistical perception into volcanic ash wt.% whereby calculated as "A", Na_2SiO_3 wt.% "B", NaOH concentration (mole) "C", Na_2SiO_3/NaOH wt.% "D", and water/binder

(w/b) wt.% "E." Table 2 shows the values for each of the five significant components. The Taguchi method study on geopolymer synthesis was used to select the values for each component tested. After determining the percentage of geopolymer paste, sand and GGBS were added to all combinations at a rate of 5 and 1.5 wt.%, respectively. Table 3 depicts the trial combination percentages and amounts utilized in the series of 16 mixtures, while Table 4 depicts the L16 array for five variables and four levels derived from the Taguchi method. Furthermore, the Taguchi method's analysis of various factors was assessed using signal-to-noise ratio (S/N) principles, representing the compressive strength values obtained from the experimental data.

Table 2. The values level and tested factors

Factor	Unit	Level 1	Level 2	Level 3	Level 4
A: Volcanic Ash	wt.%	15	20	25	30
B: Na_2SiO_3	wt.%	1	2	3	4
C: NaOH	mole	8	10	12	14
D: Na_2SiO_3/ NaOH	wt.%	1.5	2	2.5	3
E: w/b	wt.%	0.55	0.56	0.57	0.58

Table 3. The experimental design of orthogonal arrays (L16) used in Taguchi technique

Trial	Factor A	Factor B	Factor C	Factor D	Factor E
T1	1	3	3	3	3
T2	3	4	2	1	3
T3	2	2	1	4	3
T4	3	3	1	2	4
T5	2	1	2	3	4
T6	3	2	4	3	1
T7	2	3	4	1	2
T8	4	1	4	2	3
T9	1	4	4	4	4
T10	1	2	2	2	2
T11	4	3	2	4	1
T12	1	1	1	1	1
T13	3	1	3	4	2
T14	4	4	1	3	2
T15	2	4	3	2	1
T16	4	2	3	1	4

Table 4. Geopolymer concrete mixtures utilizing Taguchi technique

Mix	VA (gr)	GGBS (gr)	Sand (gr)	Na_2SiO_3 (gr)	NaOH (gr)	H_2O (gr)
T1	109.98	436.58	817.62	256.62	42.90	92.53
T2	139.28	415.62	830.14	218.24	49.66	82.24
T3	111.06	440.92	825.76	185.83	64.35	103.90
T4	165.22	384.04	821.68	208.99	56.60	92.50
T5	83.17	466.14	821.75	223.86	46.74	87.53
T6	137.86	411.35	821.59	188.18	53.70	116.17
T7	110.54	438.81	821.80	235.01	34.23	88.10
T8	137.18	409.33	817.55	211.57	42.18	108.25
T9	82.77	463.83	817.67	237.91	43.09	81.07
T10	83.58	468.47	825.85	206.38	46.76	100.98
T11	166.93	388.01	830.19	229.11	38.39	82.67
T12	84.00	470.80	829.97	183.46	46.43	120.18
T13	138.59	413.54	825.97	232.07	42.35	79.75
T14	166.07	386.02	825.92	221.06	37.64	95.45
T15	111.64	443.22	830.07	203.74	51.11	95.26
T16	164.38	382.07	817.46	190.50	60.17	111.31

2.3. Geopolymer Synthesis

The geopolymerization of volcanic ash from Mount Sinabung was accomplished by combining each material and alkaline activator. Mount Sinabung volcanic ash was used as the source material or precursor, while the alkaline activator was created using Na_2SiO_3, NaOH concentrations, and combinations of both chemicals. The concentrations of 8, 10, 12, and 14 M NaOH were obtained by dilution with distilled water. The solution was sealed and stirred for 3 h to minimize geopolymer reaction interventions while the procedure was performed until an ambient temperature and a humidity of 28°C and 75% RH were achieved during the mixing phase. As shown in Table 4, Na_2SiO_3 was added to the beaker without further preparation and stirred for 2 min, while water was added during the mixing phase before adding sand. A compact product was produced as per ASTMC109 [27] by pouring the combined solution in two layers into 50x50x50 mm molds and then vibrating them for 15 min. The specimens were covered in cling film for 1 hour to avoid moisture evaporation leaks. Afterward, the specimens were subjected to high temperature curing at 75°C for 48 h to promote the geopolymerisation process. The specimens were then allowed to cool, demolded, and stored at 28°C with 75% RH before being tested after 3, 14, and 28 days of curing.

2.4. Specimen Analysis

Per ASTM C109M [27], three specimens from each combination and a total of 48 specimens were evaluated for the compressive strength test using Compression Test Machine (Penang, Malaysia), as shown in Figure 3. SEM (Massachusetts, USA) and XRD (Massachusetts, USA) analyses were also used carried out to investigate the Mount Sinabung volcanic ash and the highest compressive strength mortar. The phase composition was determined using a Bruker D8 Advance XRD with Cu Kα radiation (1.5406) for 10 to 90 degrees of 2θ, with the results analyzed by Expert High Score Plus. Meanwhile, the morphological attributes of the volcanic ash and mortar surface was observed using SEM via Pro Suite. At an accelerating voltage of 15 kV, a focused electron beam was used to capture images with a scanning magnification of 2000x.


Figure 3. Compressive strength test process for geopolymer mortar

3. Results and Discussion

Table 5 exhibits the compressive strength results of the 16 trial mixtures proposed by the Taguchi method. The compressive strength of the various trial mixtures was determined by averaging the results of three specimen tests conducted at a particular curing time. Moreover, the optimum compressive strength for each trial mixture was formulated by averaging the values from 3, 14, and 28 days. Figure 4 demonstrates that the highest compressive strength of 73.83 MPa was generated from T5, i.e., A2B1C2D3E4, while T16, i.e., A4B2C3D2E1, produced the lowest strength of 42.14 MPa. The compressive strength of this geopolymer is greater than that of geopolymers derived from other sources, such as volcanic ash (±39 MPa) [28], GGBFS (±62 MPa) [23], Fly ash (±69 MPa) [29], GGBFS/Fly ash (±49 MPa) [30], and Treated Palm Oil Fuel Ash (±47 MPa) [22]. The test results demonstrated that the compressive strength of geopolymer mortar made from volcanic ash from Sinabung is comparable to that of other resources derived from industrial waste. However, a complete analysis of each Taguchi factor cannot be interpreted using the same analysis; thus, an additional explanation must be proposed.

Table 5. Compressive strength response of trial mixtures

Trial Mix	Combination	Compressive strength (MPa)			Compressive strength (MPa)
		Response 1	Response 2	Response 3	
		3 days	14 days	28 days	
T1	A1B3C3D3E3	74.01	65.55	64,34	69.78
T2	A3B4C2D1E3	56.37	60.62	53,11	58.49
T3	A2B2C1D4E3	50.24	52.58	59,46	51.41
T4	A3B3C1D2E4	58.11	54.89	60,64	56.50
T5	A2B1C2D3E4	79.62	68.05	66,85	73.83
T6	A3B2C4D3E1	61.19	48.34	47.15	52.22
T7	A2B3C4D1E2	68.97	57.94	49,02	63.45
T8	A4B1C4D2E3	54.34	52.73	47,55	53.53
T9	A1B4C4D4E4	76.7	60.56	52.03	63.09
T10	A1B2C2D2E2	63.06	72.12	56,70	67.59
T11	A4B3C2D4E1	60.33	57.49	69,45	58.91
T12	A1B1C1D1E1	62.72	57.23	49,82	59.97
T13	A3B1C3D4E2	60.75	74.25	69,01	67.50
T14	A4B4C1D3E2	50.22	52.89	54,30	51.55
T15	A2B4C3D2E1	57.18	48.48	55,25	52.83
T16	A4B2C3D1E4	41.93	42.36	47,87	42.14
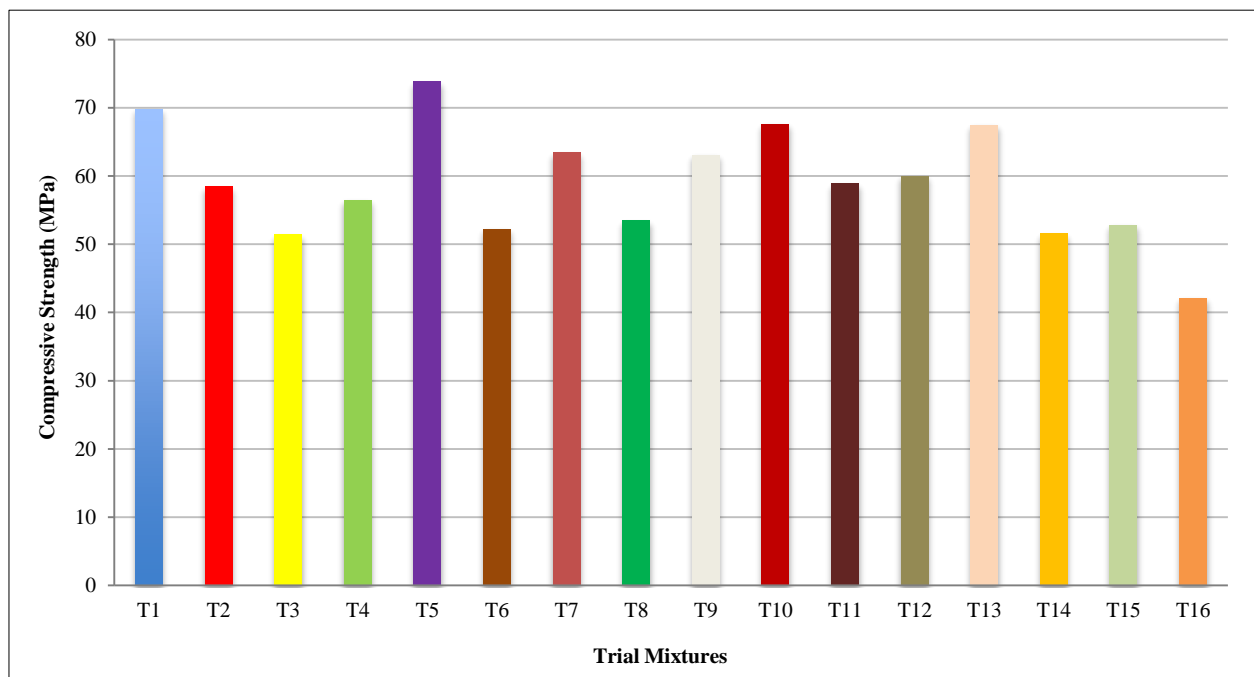
Figure 4. The average compressive strength for various trial mixtures

The Taguchi method analysis evaluates the optimal mixtures for each factor while simultaneously determining the impact on compressive strength values for Mount Sinabung ash-geopolymer mortar. For example, the compressive strength of factor A1 was tested on trial mixtures labeled T, T9, T10, and T12. Hence, the compressive strength three days after curing was the average value for trial mixtures of T1, T9, T10, and T12. Similar calculations were performed for various factors of A, B, C, D, and E, at 3, 14, and 28 days, respectively. Figure 5 depicts the compressive strength of various factors at various ages of curing on a single graph. In addition, statistical analysis based on the S/N ratio from Taguchi method data was conducted to identify the greatest impact of factors towards the compressive strength results of the mortars, to this end, a detailed discussion is provided in the following subsections.
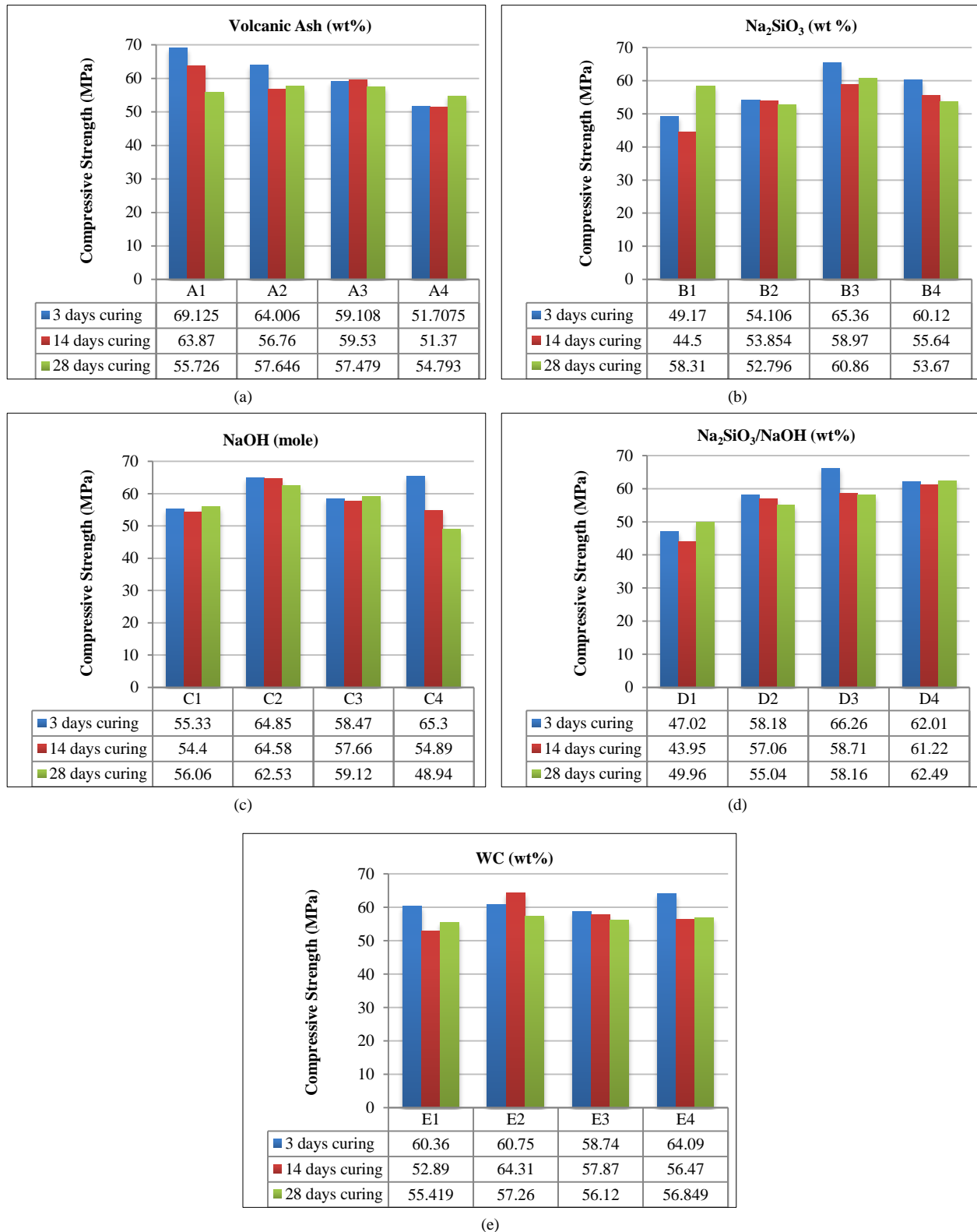
(a) Volcanic Ash (wt%)

	A1	A2	A3	A4
3 days curing	69.125	64.006	59.108	51.7075
14 days curing	63.87	56.76	59.53	51.37
28 days curing	55.726	57.646	57.479	54.793

(b) Na_2SiO_3 (wt %)

	B1	B2	B3	B4
3 days curing	49.17	54.106	65.36	60.12
14 days curing	44.5	53.854	58.97	55.64
28 days curing	58.31	52.796	60.86	53.67

(c) NaOH (mole)

	C1	C2	C3	C4
3 days curing	55.33	64.85	58.47	65.3
14 days curing	54.4	64.58	57.66	54.89
28 days curing	56.06	62.53	59.12	48.94

(d) Na_2SiO_3/NaOH (wt%)

	D1	D2	D3	D4
3 days curing	47.02	58.18	66.26	62.01
14 days curing	43.95	57.06	58.71	61.22
28 days curing	49.96	55.04	58.16	62.49

(e) WC (wt%)

	E1	E2	E3	E4
3 days curing	60.36	60.75	58.74	64.09
14 days curing	52.89	64.31	57.87	56.47
28 days curing	55.419	57.26	56.12	56.849

Figure 5. Effect of (a) Volcanic ash wt.%, (b) Na_2SiO_3 wt.%, (c) NaOH (in terms of molar), (d) Na_2SiO_3 /NaOH wt.%, (e) w/b wt.% on each response of compressive strength at different curing ages

3.1. Effect of Additive Materials

3.1.1. Effect of Mount Sinabung Volcanic Ash (Factor A)

The compressive strength for Factor A is shown in Figure 5-a. The response value reduced with the increase of Factor A1 up to A4. The response values of A1 show the highest compressive strength of 69.12 MPa, while the lowest compressive strength of 51.37 MPa was generated from A4. The highest compressive strength was observed after three days of curing, while the lowest occurred after 14 days. This result indicated that the amount of higher volcanic ash

reduced the mechanical properties of geopolymer mortar, resulting in several microcracks formations affecting the compressive strength result. According to other studies, higher amounts of volcanic glass content in a geopolymer mortar-based volcanic ash mineral product negatively affect the compressive strength [31, 32]. On the other hand, the lower amount of volcanic ash indicated a more compact structure and reduced pore availability due to a better dissolution of aluminosilicates, resulting in higher compressive strength. Meanwhile, the highest compressive strength at early ages was influenced by the CaO content of volcanic ash, affecting geopolymers' hardening time and strength [32].

3.2. Effect of Alkaline Activator Concentrations and Combinations

3.2.1. Effect of Na_2SiO_3 (Factor B)

The compressive strength for Factor B is shown in Figure 5-b, where the values improved with the increment of Factor B and began to decrease for higher values than B3. The addition of B3 demonstrated the highest compressive strength at three days (65.36 MPa), while the lowest compressive strength of 44.55 MPa was generated from B1 at 14 days. It was expected that addition of Factor B to Mount Sinabung volcanic ash-based geopolymer mortar mixtures would increase the response value. The addition of Na_2SiO_3 aims to increase the dissolved Si species so that there will be sufficient oligomeric silicates to react and form N-A-S-H gel. The lower amount of Na_2SiO_3 results in a lower compressive strength due to the lower amount of dissolved Si as SiO_4 monomer, whereas the higher amount of Na_2SiO_3 results in an increase in compressive strength due to an excess of dissolved Si species. In addition, the formation of N-A-S-H gel at a higher amount of Na_2SiO_3 also affecting the compressive strength values. However, the increased amount of Na_2SiO_3 reduced the amount of AlO_4, resulting in a geopolymer that hardens more quickly, resulting in greater compressive strength at early curing time.

3.2.2. Effect of NaOH (Factor C)

Figure 5-c depicts the compressive strength of Factor C, where the highest response value at three days of curing time was generated by C2 (65.30 MPa), and C4 generated the lowest value at 28 days of curing time. The increase of factor C up to C2 enhanced the compressive strength value while the addition of higher than C2 reduced the compressive strength. NaOH solution is an activating solution that functions to dissolve Si and Al, fulfilling the required amount for the geopolymerization process producing SiO_4 and AlO_4 monomers. The higher amount of volcanic ash and Na_2SiO_3 lead to a greater amount of NaOH solution to optimally dissolve Si and Al. However, the higher concentration of NaOH produced an excess of Na^+ species that altered the balance requirement within the structure by satisfying the sodium content attraction, resulting in a decrease in compressive strength. On the other hand, the quantity of OH- groups that inhibit geopolymerization were attracted to initiate the dissolution of aluminosilicate minerals, resulting in broken Si-O-Si, Al-O-Al, and Si-O-Al and the formation of Al-OH and Si-OH groups [33]. These phenomena resulted in the formation of CSH gel binder and increased porosity, which influenced compressive strength values.

3.2.3. Effect of Na_2SiO_3/NaOH (Factor D)

The compressive strength for Factor D is shown in Figure 5-d, where the highest compressive strength was generated by D3 (66.26 MPa), and D1 exhibited the lowest (43.95 MPa). It was observed that the peak compressive strength occurred after three days of curing, whereas the lowest occurred after 14 days. The trend results were generally consistent with those of previous studies [22, 34]. Incorporating Factor D into the activating solutions improves the polymerization of the ionic species present in the system, increasing compressive strength. The enhanced value resulted from increased $[SiO_4]^{4-}$ concentrations, which accelerated the polymerization reaction rate. In contrast, a smaller quantity of Na_2SiO_3 decreases the silica concentration during the polymerization process, resulting in a less polymerized distribution of silicon species and a corresponding reduction in compressive strength. This distinction was due to the rate of influence on compressive strength resulting from the production of C–S–H and geopolymer (N-A–S–H) gels as the amorphous silica content increased [22].

3.2.4. Effect of w/b (Factor E)

The compressive strength for Factor E is shown in Figure 5-e, where response values improved with Factor E increases up to E4. The addition of Factor E4 resulted in the highest compressive strength (64.09 MPa) at three days, while the lowest of 52.89 MPa was generated from E1 at 14 days. This is possible because increasing the activator concentration in the mixture necessitates increasing the water concentration, as it is well known that geopolymer processes heavily rely on polymerization and condensation. This phenomenon is less obvious because it is necessary to provide sufficient water by increasing the water/binder ratio to facilitate mixing and ionic transport. Moreover, excess water may dilute the reaction or drain the more soluble components away from the reaction zone, resulting in a greater polymerization process that influences compressive strength [34, 35].

3.3. The Analysis of Signal-to-noise (S/N) Ratio based on Taguchi Method Result

The S/N ratio analysis of the Taguchi method provides the highest compressive strength values for Mount Sinabung volcanic ash-geopolymer mortar while determining the optimal impact of all factors. Greater levels of S/N ratio indicate the controlling factor settings that limit the impacts of noise factors value. Delta represents the difference between the highest and minimum average S/N ratios for each factor, whereby a larger Delta indicates a bigger influence on compressive strength mortar. The S/N ratio of various factors was analyzed using Minitab software, depicted in Figure 6 and Table 6. It was observed that the highest mean S/N ratio was generated from 1 wt.% Na_2SiO_3, reaching a value of 36.44 while the lowest produced from 4 wt.% (34.23). Meanwhile, Na_2SiO_3/NaOH exhibits the highest value of 35.41 and the lowest of 34.90 for the mean S/N ratio. Based on these data, the Delta of Na_2SiO_3 was formulated, generating 2.21 as the highest while the lowest delta value of 0.51 from Na_2SiO_3/NaOH. This result characterizes the novelty of the present study, where Na_2SiO_3 exhibits the greatest impact on geopolymer mortar mixtures while the weakest impact is generated from Na_2SiO_3/NaOH. This was explained by the fact that the presence of Na_2SiO_3 compensates for the lack of silica in the volcanic ash of Mount Sinabung, causing sufficient oligomeric silicates to react and form N-A-S-H gel. Consequently, Na_2SiO_3 is essential as an activator in the production of hydration products and geopolymeric binders that influence the microstructure of geopolymer mortar. In contrast, the increased Na_2SiO_3/NaOH weight percent had a negligible effect because other factors, such as the excess presence of Na^+ and decreased silica concentration during the mixing process, dominated the polymerization events.
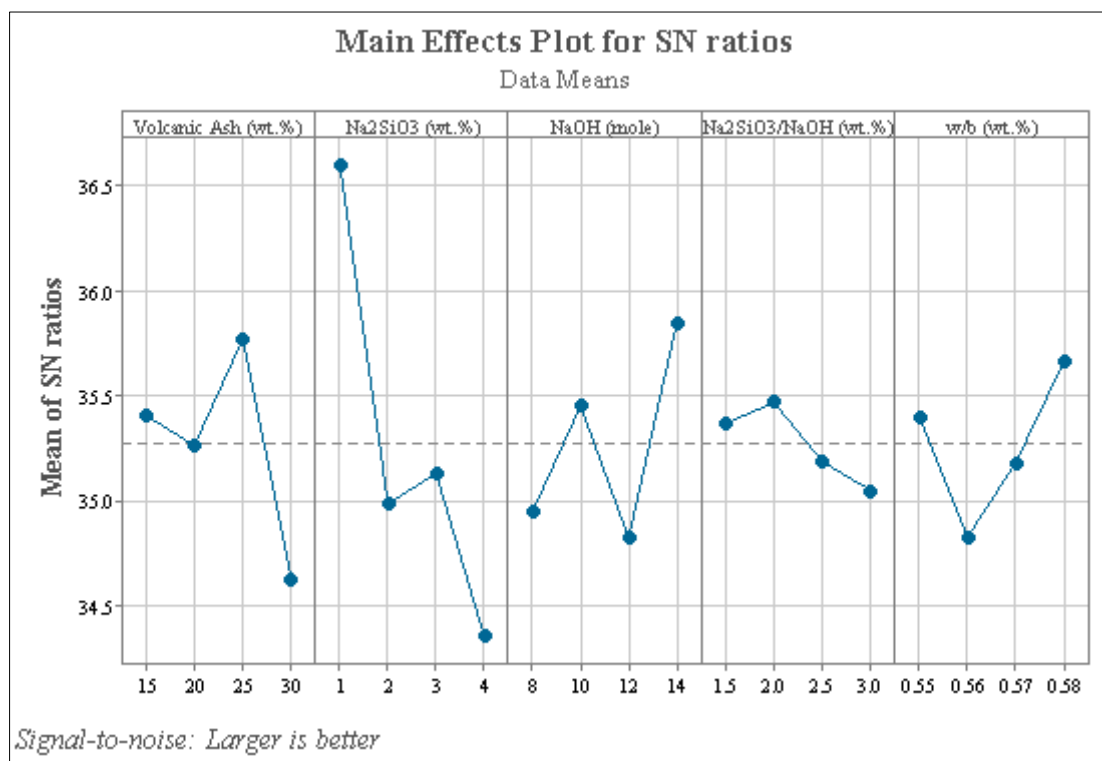

Figure 6. The signal to noise (SN) ratio graph for each factor in Taguchi design

Table 6. The signal to noise (SN) ratio value for each factor in Taguchi design

Level	Volcanic Ash	Na_2SiO_3	NaOH	Na_2SiO_3/NaOH	w/b
1	35.46	36.44	34.81	35.27	35.31
2	35.17	34.81	35.32	35.41	34.62
3	35.65	34.92	34.7	35.13	35.03
4	34.64	34.23	35.73	34.9	35.58
Delta	1.01	2.21	1.03	0.51	0.96

3.4. Characterization of Mount Sinabung Volcanic Ash-Based Geopolymer Mortar

3.4.1. SEM Analysis

Figure 7-a shows the SEM image of volcanic ash particles from Mount Sinabung as berry-like glass particles with angular, blocky shapes, low vesicularity, and crystallized plagioclase. This texture exists on all sizes of glass beads and glass layers representing the aluminosilicate type, while numerous shards and a big hollow are revealed in a sharp and

jagged form, representing the amorphous phase. These observations are supported by the XRF result from Mount Sinabung volcanic ash, which shows several aluminosilicates' constituents. Furthermore, the Mount Sinabung volcanic ash geopolymer morphology from T5 mortar mixtures (A2B1C2D3E4) is evident in Figure 7-b. Numerous flakes were arranged into solid structures, while the geopolymer mortar's surface exhibited minimal porosity, indicating a compact structure. The hydration product of N-A-S-H and C-S-H was formed, attributed to small granular bodies contacting each other, and suspended in a lamellar matrix [36, 37]. These assumptions corresponded with the high compressive strength results from T5 mortar mixtures (A2B1C2D3E4).
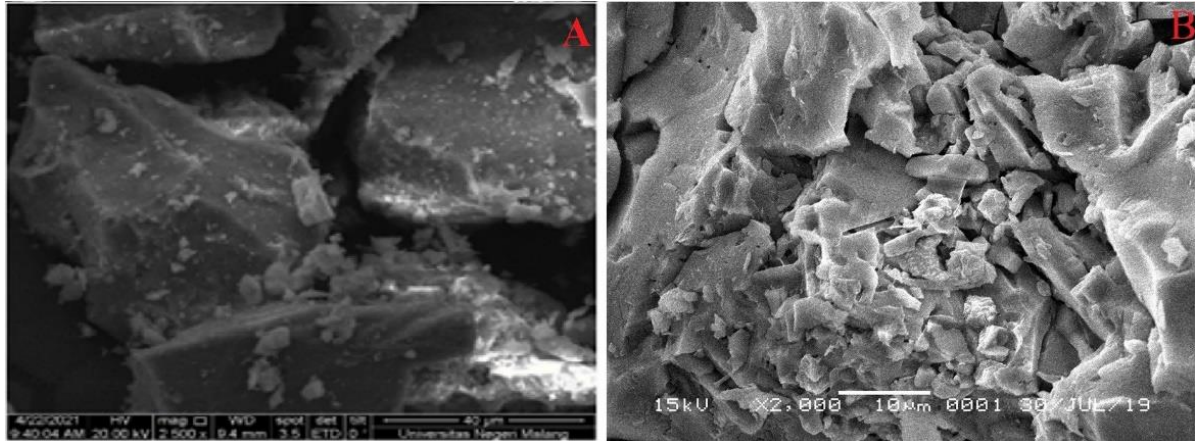
Figure 7. SEM of Sinabung volcanic ash (a) and geopolymer mortar (b)

3.4.2. XRD Analysis

The results of XRD patterns are presented in Figure 8; Sinabung volcanic ash (a) and T5 mixtures (A2B1C2D3E4) from geopolymer mortar (b) are identified using the XPert High Score Software. The intensity of peaks obtained from Mount Sinabung volcanic ash samples show crystalline phases, i.e., quartz, cristobalite, alunite, anorthite, and maghemite. This result proved the potential of Mount Sinabung volcanic ash as a natural resource that can be substituted with OPC as a binder to form concrete. The crystalline phase analysis agrees with the XRF result representing aluminosilicate. Another researcher made a similar analysis [38, 39]. Its diffractogram changed when several activators activated the original Sinabung volcanic ash to form geopolymer mortar. The original mineralogy of Sinabung volcanic ash was not significantly altered for the geopolymer pattern. The initial material observed the crystalline phases of quartz, cristobalite, alunite, anorthite, and maghemite, whereas calcite, albite, and akermanite were formed in calcite, albite, and akermanite geopolymer mortar. This change indicates the formation of aluminosilicate hydrate gel, which has been identified as the N-A-S-H and C-S-H formation phases, resulting in an increase in the compressive strength of the mortar and a denser microstructure of the sample [4, 36].
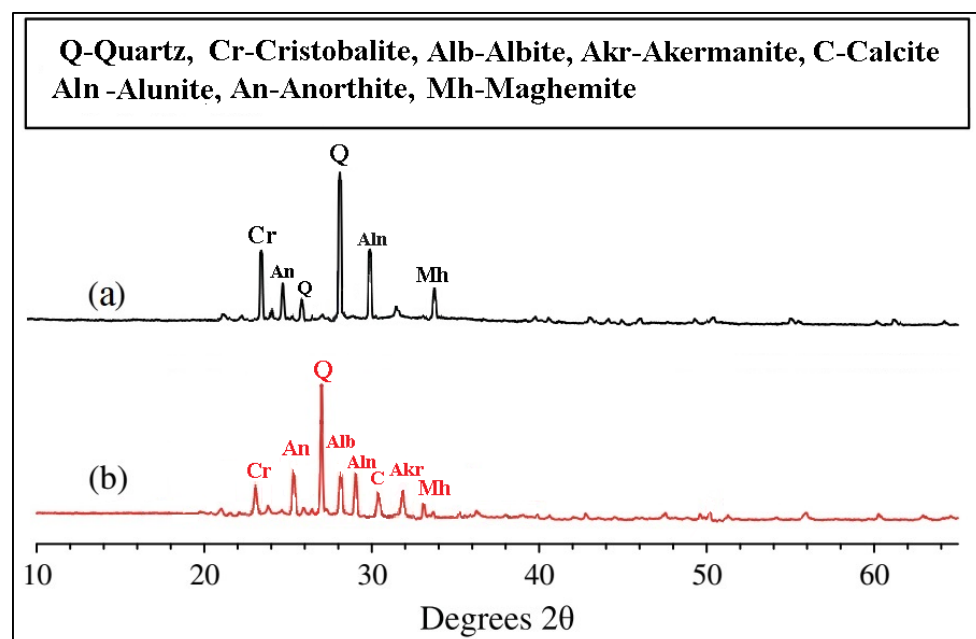

Figure 8. X-ray diffractograms of Sinabung Volcanic Ash (a) and geopolymer mortar (b)

4. Conclusion

This study demonstrated that Mount Sinabung volcanic ash was successfully utilized as a natural resource to produce geopolymer mortar. The Taguchi experimental design method was utilized as a useful statistical method for evaluating five design elements in a single work that produces an L16 array. The T5 trial mixture, i.e., A2B1C2D3E4, yielded the highest compressive strength value of 79.62 MPa after three days of curing, while the T16 trial mixture, i.e., A4B2D1E1E4, yielded the lowest compressive strength value of 41.93 MPa after three days. The optimal specific mixtures of A2B1C2D3E4 are generated from 20 wt.% Mount Sinabung volcanic ash, 1 wt.% of Na_2SiO_3, 10 moles of NaOH, 12 wt.% Na_2SiO_3/ NaOH and 0.58 wt.% w/b, while A4B2C3D1E4 consists of 30 wt.% Mount Sinabung volcanic ash, 2 wt.% of Na_2SiO_3, 12 mole NaOH, 1.5 wt.% Na_2SiO_3/ NaOH and 0.58 wt.%. Furthermore, the result of the S/N ratio indicated that Na_2SiO_3 had the greatest impact on compressive strength, while Na_2SiO_3/NaOH had the lowest impact. The high compressive strength resulted from forming a dense and compact microstructure with small voids on the surface, as demonstrated by SEM results, whereas volcanic ash was found to have a sharp and jagged form, indicating an amorphous phase and aluminosilicate type. In addition, the XRD result from Mount Sinabung volcanic ash indicated a crystalline phase, i.e., quartz, cristobalite, alunite, anorthite, and maghemite, whereas the geopolymer mortar result shows a formation of gel binders such as N-A-S-H and C-S-H. Therefore, this study demonstrates a potential solution for materials other than OPC, producing geopolymers that conserve natural resources and protect the environment by diverting waste.

5. Declarations

5.1. Author Contributions

Conceptualization, R.K. and J.T.; methodology, R.K.; software, R.K.; validation, R.K. and H.H.; formal analysis, R.K.; investigation, R.K.; resources, R.K.; data curation, R.K.; writing—original draft preparation, R.K.; writing—review and editing, M.J. and M.A.; visualization, H.H. and M.J.; supervision, J.T., M.J., M.A., and H.H.; project administration, R.K.; funding acquisition, R.K. and J.T. All authors have read and agreed to the published version of the manuscript.

5.2. Data Availability Statement

The data presented in this study are available in article.

5.3. Funding and Acknowledgements

5.4. Conflicts of Interest

The authors declare no conflict of interest.

6. References

[1] Alberto, F., Guerreiro, M.S. (2021). World Business Council for Sustainable Development. Encyclopaedia of Sustainable Management. Springer, Cham, Switzerland. doi:10.1007/978-3-030-02006-4_974-1.

[2] Cadavid-Giraldo, N., Velez-Gallego, M. C., & Restrepo-Boland, A. (2020). Carbon emissions reduction and financial effects of a cap and tax system on an operating supply chain in the cement sector. Journal of Cleaner Production, 275, 122583. doi:10.1016/j.jclepro.2020.122583.

[3] Di Filippo, J., Karpman, J., & DeShazo, J. R. (2019). The impacts of policies to reduce CO2 emissions within the concrete supply chain. Cement and Concrete Composites, 101, 67–82. doi:10.1016/j.cemconcomp.2018.08.003.

[4] Mehta, A., Siddique, R., Singh, B. P., Aggoun, S., Łagód, G., & Barnat-Hunek, D. (2017). Influence of various parameters on strength and absorption properties of fly ash based geopolymer concrete designed by Taguchi method. Construction and Building Materials, 150, 817–824. doi:10.1016/j.conbuildmat.2017.06.066.

[5] Topçu, I. B., Toprak, M. U., & Uygunoǧlu, T. (2014). Durability and microstructure characteristics of alkali activated coal bottom ash geopolymer cement. Journal of Cleaner Production, 81, 211–217. doi:10.1016/j.jclepro.2014.06.037.

[6] Yang, G., Zhao, J., & Wang, Y. (2022). Durability properties of sustainable alkali-activated cementitious materials as marine engineering material: A review. Materials Today Sustainability, 17, 100099. doi:10.1016/j.mtsust.2021.100099.

[7] Davidovits, J. (2013). Geopolymer cement. A review. Technical papers, 21, Geopolymer Institute, Saint-Quentin, France.

[8] Glukhovsky, V. D. (1959). Soil silicates (Gruntosilikaty). Budivelnik Publication, Kyiv, Ukraine.

[9] Juenger, M. C. G., Winnefeld, F., Provis, J. L., & Ideker, J. H. (2011). Advances in alternative cementitious binders. Cement and Concrete Research, 41(12), 1232–1243. doi:10.1016/j.cemconres.2010.11.012.

[10] Scrivener, K. L., John, V. M., & Gartner, E. M. (2018). Eco-efficient cements: Potential economically viable solutions for a low-CO2 cement-based materials industry. Cement and Concrete Research, 114, 2–26. doi:10.1016/j.cemconres.2018.03.015.

[11] Ganeshan, M., & Venkataraman, S. (2022). Interface shear strength evaluation of self-compacting geopolymer concrete using push-off test. Journal of King Saud University - Engineering Sciences, 34(2), 98–107. doi:10.1016/j.jksues.2020.08.005.

[12] Onoue, K., Iwamoto, T., & Sagawa, Y. (2019). Optimization of the design parameters of fly ash-based geopolymer using the dynamic approach of the Taguchi method. Construction and Building Materials, 219, 1–10. doi:10.1016/j.conbuildmat.2019.05.177.

[13] Lin, R. S., Han, Y., & Wang, X. Y. (2021). Experimental study on optimum proportioning of Portland cements, limestone, metakaolin, and fly ash for obtaining quaternary cementitious composites. Case Studies in Construction Materials, 15. doi:10.1016/j.cscm.2021.e00691.

[14] Chindaprasirt, P., Jitsangiam, P., Chalee, W., & Rattanasak, U. (2021). Case study of the application of pervious fly ash geopolymer concrete for neutralization of acidic wastewater. Case Studies in Construction Materials, 15, 770. doi:10.1016/j.cscm.2021.e00770.

[15] Kumar, G., & Mishra, S. S. (2021). Effect of GGBFS on workability and strength of alkali-activated geopolymer concrete. Civil Engineering Journal, 7(6), 1036–1049. doi:10.28991/cej-2021-03091708.

[16] Aziz, A., Benzaouak, A., Bellil, A., Alomayri, T., Ni el Hassani, I. E. E., Achab, M., El Azhari, H., Et-Tayea, Y., & Shaikh, F. U. A. (2021). Effect of acidic volcanic perlite rock on physio-mechanical properties and microstructure of natural pozzolan based geopolymers. Case Studies in Construction Materials, 15, 712. doi:10.1016/j.cscm.2021.e00712.

[17] Robayo-Salazar, R. A., & Mejía de Gutiérrez, R. (2018). Natural volcanic pozzolans as an available raw material for alkali-activated materials in the foreseeable future: A review. Construction and Building Materials, 189, 109–118. doi:10.1016/j.conbuildmat.2018.08.174.

[18] Tchakoute Kouamo, H., Elimbi, A., Mbey, J. A., Ngally Sabouang, C. J., & Njopwouo, D. (2012). The effect of adding alumina-oxide to metakaolin and volcanic ash on geopolymer products: A comparative study. Construction and Building Materials, 35, 960–969. doi:10.1016/j.conbuildmat.2012.04.023.

[19] de Jong, B. H. W. S., & Brown, G. E. (1980). Polymerization of silicate and aluminate tetrahedra in glasses, melts, and aqueous solutions-I. Electronic structure of H6Si2O7, H6AlSiO71-, and H6Al2O72-. Geochimica et Cosmochimica Acta, 44(3), 491–511. doi:10.1016/0016-7037(80)90046-0.

[20] Duxson, P., Provis, J. L., Lukey, G. C., Mallicoat, S. W., Kriven, W. M., & Van Deventer, J. S. J. (2005). Understanding the relationship between geopolymer composition, microstructure and mechanical properties. Colloids and Surfaces A: Physicochemical and Engineering Aspects, 269(1–3), 47–58. doi:10.1016/j.colsurfa.2005.06.060.

[21] He, J., Zhang, J., Yu, Y., & Zhang, G. (2012). The strength and microstructure of two geopolymers derived from metakaolin and red mud-fly ash admixture: A comparative study. Construction and Building Materials, 30, 80–91. doi:10.1016/j.conbuildmat.2011.12.011.

[22] Mijarsh, M. J. A., Megat Johari, M. A., & Ahmad, Z. A. (2014). Synthesis of geopolymer from large amounts of treated palm oil fuel ash: Application of the Taguchi method in investigating the main parameters affecting compressive strength. Construction and Building Materials, 52, 473–481. doi:10.1016/j.conbuildmat.2013.11.039.

[23] Hadi, M. N. S., Farhan, N. A., & Sheikh, M. N. (2017). Design of geopolymer concrete with GGBFS at ambient curing condition using Taguchi method. Construction and Building Materials, 140, 424–431. doi:10.1016/j.conbuildmat.2017.02.131.

[24] He, J., Jie, Y., Zhang, J., Yu, Y., & Zhang, G. (2013). Synthesis and characterization of red mud and rice husk ash-based geopolymer composites. Cement and Concrete Composites, 37(1), 108–118. doi:10.1016/j.cemconcomp.2012.11.010.

[25] Nazari, A., Riahi, S., & Bagheri, A. (2012). Designing water resistant lightweight geopolymers produced from waste materials. Materials and Design, 35, 296–302. doi:10.1016/j.matdes.2011.09.016.

[26] Riahi, S., Nazari, A., Zaarei, D., Khalaj, G., Bohlooli, H., & Kaykha, M. M. (2012). Compressive strength of ash-based geopolymers at early ages designed by Taguchi method. Materials and Design, 37, 443–449. doi:10.1016/j.matdes.2012.01.030.

[27] Calderón, N., Vargas, M., Almirón, J., Bautista, A., Velasco, F., & Tupayachy-Quispe, D. (2021). Influence of the Activating Solution and Aggregates in the Physical and Mechanical Properties of Volcanic Ash Based Geopolymer Mortars. IOP Conference Series: Materials Science and Engineering, 1054(1), 012003. doi:10.1088/1757-899x/1054/1/012003.

[28] ASTM C109/C109M-20. (2020). Standard Test Method for Compressive Strength of Hydraulic Cement Mortars (Using 2-in. or [50-mm] Cube Specimens). ASTM International, Pennsylvania, United States. doi:10.1520/C0109_C0109M-20.

[29] Olivia, M., & Nikraz, H. (2012). Properties of fly ash geopolymer concrete designed by Taguchi method. Materials & Design (1980-2015), 36, 191–198. doi:10.1016/j.matdes.2011.10.036.

[30] Mehta, A., Siddique, R., Ozbakkaloglu, T., Uddin Ahmed Shaikh, F., & Belarbi, R. (2020). Fly ash and ground granulated blast furnace slag-based alkali-activated concrete: Mechanical, transport and microstructural properties. Construction and Building Materials, 257, 119548. doi:10.1016/j.conbuildmat.2020.119548.

[31] Shoji, S., Kodayashi, S., Yamada, I., & Masui, J. (1975). Chemical and mineralogical studies on volcanic ashes I. Chemical composition of volcanic ashes and their classification. Soil Science and Plant Nutrition, 21(4), 311–318. doi:10.1080/00380768.1975.10432646.

[32] Ilham, D. J., Anggarini, U., Juniarti, J., & Fiantis, D. (2021). Utilization of volcanic ashes for geopolymer based on alkaline activator and solid-liquid ratio. IOP Conference Series: Earth and Environmental Science, 708(1), 012058. doi:10.1088/1755-1315/708/1/012058.

[33] Tashima, M. M., Soriano, L., Borrachero, M. V., Monzó, J., & Payá, J. (2013). Effect of curing time on microstructure and mechanical strength development of alkali activated binders based on vitreous calcium aluminosilicate (VCAS). Bulletin of Materials Science, 36(2), 245–249. doi:10.1007/s12034-013-0466-z.

[34] Pacheco-Torgal, F., Moura, D., Ding, Y., & Jalali, S. (2011). Composition, strength and workability of alkali-activated metakaolin based mortars. Construction and Building Materials, 25(9), 3732–3745. doi:10.1016/j.conbuildmat.2011.04.017.

[35] Barbosa, V. F. F., MacKenzie, K. J. D., & Thaumaturgo, C. (2000). Synthesis and characterisation of materials based on inorganic polymers of alumina and silica: Sodium polysialate polymers. International Journal of Inorganic Materials, 2(4), 309–317. doi:10.1016/S1466-6049(00)00041-6.

[36] Ghadir, P., & Razeghi, H. R. (2022). Effects of sodium chloride on the mechanical strength of alkali activated volcanic ash and slag pastes under room and elevated temperatures. Construction and Building Materials, 344, 128113. doi:10.1016/j.conbuildmat.2022.128113.

[37] Bellum, R. R., Muniraj, K., & Madduru, S. R. C. (2020). Influence of slag on mechanical and durability properties of fly ash-based geopolymer concrete. Journal of the Korean Ceramic Society, 57(5), 530–545. https://doi.org/10.1007/s43207-020-00056-7.

[38] Latif, D. O. (2016). Chemical Characteristics of Volcanic Ash in Indonesia for Soil Stabilization: Morphology and Mineral Content. International Journal of Geomate. doi:10.21660/2016.26.151120.

[39] Sinuhaji, P., Sembiring, T., Magfirah, A., Piliang, A. F., & Nababan, S. M. (2018). Analysis of Composition; Topography of Volcanic Materials Erupted from Mount Sinabung, Karo Regency, Indonesia. Journal of Physics: Conference Series, 1116(3), 32035. doi:10.1088/1742-6596/1116/3/032035.